Cu-incorporated mesoporous materials: Synthesis, characterization and catalytic activity in phenol hydroxylation

Huili Tang, Yu Ren, Bin Yue *, Shirun Yan, Heyong He *

*Department of Chemistry and Shanghai Key Laboratory of Molecular Catalysis and Innovative Materials,
Fudan University, Shanghai 200433, PR China*

Abstract

A series of novel Cu-incorporated mesoporous materials (CMMs) with molar ratios of Cu/Si ranging from 1/200 to 1/20 were synthesized by sol–gel method using glutaric acid as template. The materials were characterized by powder X-ray diffraction (XRD), N_2 adsorption, diffuse reflectance UV–vis spectroscopy and transmission electron microscopy (TEM). The results indicate that the CMMs have a three-dimensional (3D) worm-like mesoporous structure with a surface area between 600 and $800 \, m^2 \, g^{-1}$ and the copper ions are incorporated into the matrix with octahedral environment. The catalytic activity of these CMMs in the phenol hydroxylation using H_2O_2 as oxidant is comparable to that of TS-1. Effects of Cu/Si molar ratio in the catalyst and the influence of various reaction parameters on the catalytic activity were investigated in detail and the optimized reaction condition was acquired.
© 2006 Elsevier B.V. All rights reserved.

Keywords: Cu-incorporated mesoporous materials; Phenol; Hydroxylation; Glutaric acid; H_2O_2

1. Introduction

Diphenols (catechol and hydroquinone) are important chemicals which have been widely used in many aspects such as photographic developers, rubber and fat antioxidants, polymerization inhibitors, antiseptic and reducing agents, and pharmaceutical intermediates, etc. The production of diphenols from hydroxylation of phenol has attracted much attention since 1970s [1]. Up to now, many homogeneous and heterogeneous catalysts have been employed in this reaction. For the homogeneous systems, water soluble metal ions, metal complexes, and polyoxometalates were used to catalyze the phenol hydroxylation with aqueous H_2O_2 and other oxidants as oxygen donors [2–4]. However, the shortcomings of homogeneous catalysts, such as difficulties in recovery, relatively poor stability and low conversion, limited their industrial applications. Therefore, development of heterogeneous catalysts is particularly attractive. It was found that various bulk metal oxides or supported oxides, e.g.,

α-Fe_2O_3/SiO_2 [5], $Cu_2(OH)PO_4$ [6] and V–Zr mixed oxides [7], exhibited catalytic activity in the hydroxlation of phenol. Transition metal ion-exchanged layer clays, such as hydrotalcite [8,9] and montmorillonite [10], were also studied for this purpose.

The hydroxylation of phenol has become a promising environmental-friendly approach since TS-1 was used as the catalyst and aqueous H_2O_2 as the oxidant [11]. Several transition metal substituted microporous zeolites, such as TS-2, Ti-β, and Fe-Co/β, have also been studied [12–14]. However, the small pore size of microporous molecular sieves may arise the diffusion problem. The advent of mesoporous silica paved a new way for designing the catalysts with larger pore size where transition metal ions, metal oxides or metal complexes can be immobilized or supported on the channel surface or incorporated into the matrix of mesoporous silicas [15–22]. Some of these mesoporous materials showed catalytic activity of phenol hydroxylation [16,18–22]. But some problems, such as complicated preparation procedure and leaching of active species, are not well-resolved. Therefore, it is necessary to develop simple motheds for preparing environmental-friendly catalysts with high stability and high catalytic activity.

* Corresponding authors. Tel.: +86 21 65643916; fax: +86 21 65642978.
E-mail addresses: yuebin@fudan.edu.cn (B. Yue), heyonghe@fudan.edu.cn
(H. He).

In our previous work, Ti^{4+}-containing mesoporous silicas which exhibited high catalytic activity in the cyclohexene epoxidation reaction were prepared by an "one-pot" method using short chain carboxylic acids as the templates [23]. Here we report synthesis and characterization of Cu-incorporated mesoporous materials CMM-*x* (*x* stands for Cu/Si molar ratio in starting materials) using glutaric acid as template and their catalytic activity in phenol hydroxylation reaction in details.

2. Experimental

2.1. Synthesis

Cu-incorporated mesoporous materials CMM-*x* with different Cu/Si molar ratios were synthesized by a sol–gel method using glutaric acid as template, copper(II) acetate as copper source, and tetraethylorthosilicate (TEOS) as silica source. Desired amounts of copper(II) acetate, glutaric acid, HCl (2 mol L^{-1}) and H_2O were stirred together. Then a desired amount of TEOS was added to form a clear solution with a molar ratio of 1.00 Si:*x* metal:0.50 glutaric acid:2 HCl:45 H_2O. After hydrolysis of TEOS for 1 h, the mixture was dried at 423 K for 2 h and a gel was obtained. Finally, the gel was calcined in air at 773 K for 5 h and the CMM-*x* catalysts were obtained. The final molar ratios of Cu/Si in the CMM samples determined by EDX are given in Table 1.

2.2. Characterization

The powder X-ray diffraction (XRD) patterns were obtained from a Rigaku D/MAX-II diffractometer with Cu Kα radiation. The BET surface areas, average pore sizes and pore volumes were determined by N_2 adsorption–desorption measurements at 77 K with a Micromeritics Tristar 3000 analyser. The pore size distributions were calculated from the desorption branch of the isotherms. The UV–vis diffuse reflectance spectra (DRS) were measured with a JASCO UV550 UV–vis absorption spectrometer. The transmission electron microscopy (TEM) images were obtained from a Jeol JEM 2011 electron microscope with a Link ISIS 300 EDX instrument. The leaching of Cu during the catalytic reaction was determined by ICP analysis on a Thermo Elemental IRIS Intrepid spectrometer. In the recycled runs, the catalyst was recovered by centrifugation and drying at 40 °C for 5 h.

2.3. Catalytic activity test

Phenol hydroxylation was carried out at 343 K in a three-necked flask (50 mL) equipped with a magnetic stirrer and a reflux condenser. Phenol, distilled water and catalyst was added successively into the flask and heated to 343 K. A 30 wt.% H_2O_2 was then added dropwisely and the reaction was carried out for a certain period of time. The mixture was centrifugated to remove the catalyst and the liquid samples were further diluted to 100 mL with deionized water before analysis. The analysis of products was carried out on an Agilent 1100 HPLC equipped with a 150 mm reversed phase C18 column at ambient temperature [24,25] and a dual wavelength UV detector (245 and 280 nm). A methanol/water mixture (30/70 vol.%, 0.8 mL min^{-1}) was used as the eluant. The conversion of phenol, the slectivity of diphenol and the product distribution are all based on molar pecentages.

3. Results and discussion

3.1. Characterization

3.1.1. X-ray diffraction

The XRD patterns of the CMMs are shown in Fig. 1. The XRD patterns of all the CMMs in the small angle region are similar to that of HMS mesoporous molecular sieve [26], showing only a broad peak in the region of 0.6–1.2°, which probably indicates the mesoporous feature. In large angle region of 10–60°, a hump at 15–30° is observed for all materials, which is from the amorphous silica. Besides the hump, CMM-1/50 and the samples with higher Cu content exhibit two weak diffractions at $2\theta = 35.3°$ and $38.5°$ assignable to ($\bar{1}$ 1 1) and (1 1 1) diffractions due to the formation of minor tenorite phase of copper oxide. CMM-1/200 and CMM-1/100 exhibit no diffraction peaks of tenorite phase, indicating that the Cu species in the matrix are well dispersed.

3.1.2. N_2 adsorption analysis

The typical N_2 adsorption isotherm of CMM-1/50 shown in Fig. 2 is of type IV classification with a H2 hysteresis loop [27]. It has a sharp inflection at p/p_0 of 0.5–0.6 and an H2 hysteresis loop at p/p_0 between 0.4 and 0.8, indicating its mesopore system. The BET surface areas, pore volumes, and average pore diameters of all CMMs are listed in Table 1. The CMMs have average pore diameter in mesoporous range with large BET surface areas (620–780 m^2 g^{-1}) and large pore volume (0.66–0.88 cm^3 g^{-1}). BET surface area of the CMMs increases but pore size and pore volume roughly decrease with decreasing the molar ratio of Cu/Si.

3.1.3. TEM measurements

The TEM images of all CMMs show worm-like mesoporous structures, which is similar to that of HMS mesoporous materials [26]. A typical TEM image of CMM-1/50 is shown in Fig. 3(a). In order to check whether the pore structure of CMMs is three-dimensional (3D), an inverse carbonaceous mesoporous material was prepared using CMM-1/50 as hard template [28]. The TEM image of carbonaceous structure (Fig. 3(b)) reflects similar inter-

Table 1
Physicochemical properties of the CMMs

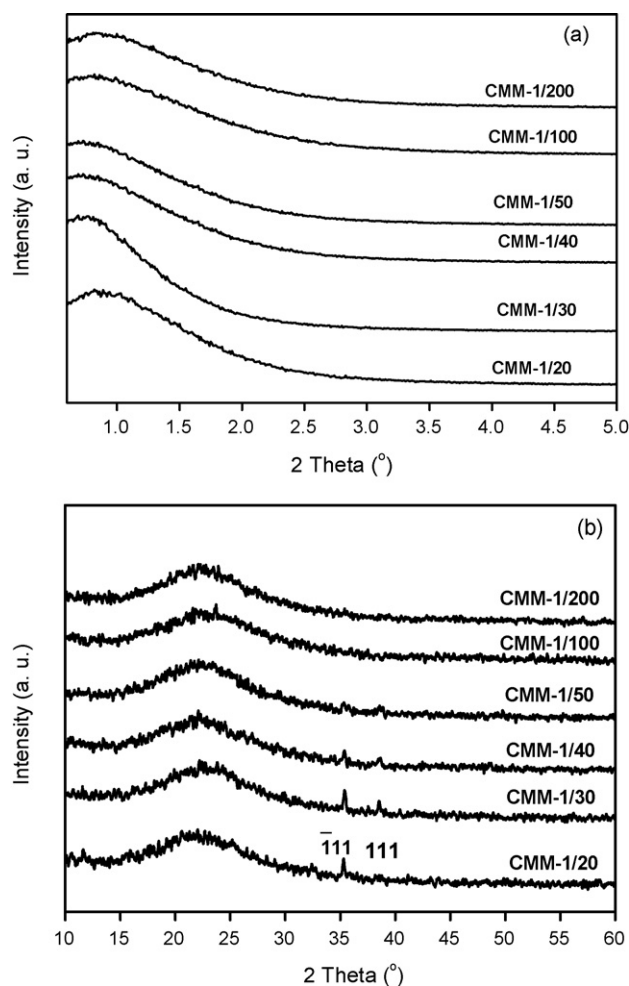| Sample	Molar ratio of Cu/Si[a]	Average pore size (nm)	Pore volume (cm^3 g^{-1})	Surface area (m^2 g^{-1})
CMM-1/20	1/19.6	5.67	0.87	624
CMM-1/30	1/30.2	5.19	0.88	698
CMM-1/40	1/39.5	4.12	0.70	701
CMM-1/50	1/49.8	3.84	0.69	726
CMM-1/100	1/98.8	3.57	0.67	770
CMM-1/200	1/196.4	3.36	0.66	780

[a] Analyzed by EDX.

Fig. 1. X-ray diffraction patterns of Cu-incorporated mesoporous materials with different Cu/Si ratios in small angle region (a) and large angle region (b).

connected mesopore network, which is inferred that the CMMs have a 3D interconnected mesopore structure [29].

3.1.4. Diffuse reflectance UV–vis spectroscopy

Fig. 4 shows the UV–vis DRS of the CMMs. All spectra have a broad absorption band in the region of 600–900 nm which can be attributed to the d–d transition of Cu(II) ion in the octahedral
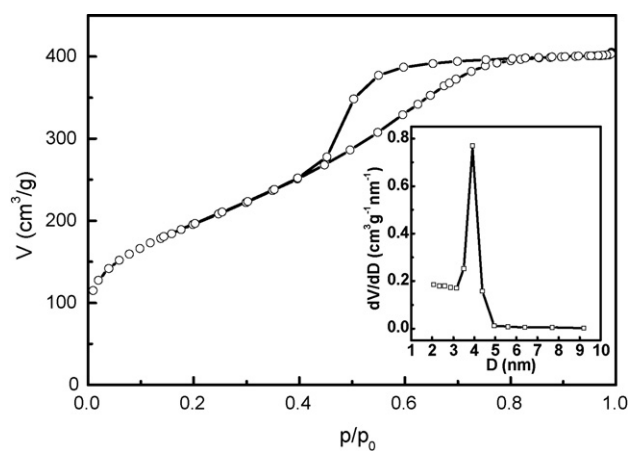

Fig. 2. Typical N_2 adsorption/desorption isotherm and pore size distribution for CMM-1/50.

ligand field generated by oxygen ions [30]. The intensity of the band at 600–900 nm increases with increasing Cu content. The band centered at ca. 250 nm may be related with the silica matrix [30]. It is noticeable that the intensity of a shoulder at ca. 320 nm assignable to the electron charge transferring from coordination oxygen ligands to central Cu(II) ions, also increases with increasing copper content in CMMs [30]. The similarity of CMMs in UV–vis spectra, along with the results of XRD, infers that the copper in the CMMs with low content mainly forms the highly dispersed Cu(II) oxide aggregates within mesoporous siliceous matrices [31].

3.2. Catalytic phenol hydroxylation over CMMs

3.2.1. The hydroxylation activity over various catalysts

The catalytic reaction data of CMMs, TS-1 and CuO catalysts in phenol hydroxylation are listed in Table 2. The non-porous bulk oxide CuO shows relatively low conversion of 9.8%. The CMMs exhibit remarkable catalytic activity, whereas the sample without Cu prepared in the similar way to CMMs shows almost no catalytic activity. Although the catalytic activity of CMMs does not change significantly with varying copper content, a phenol conversion of 25.1% is observed for CMM-1/50, which is comparable to that of TS-1 [32]. The excellent catalytic
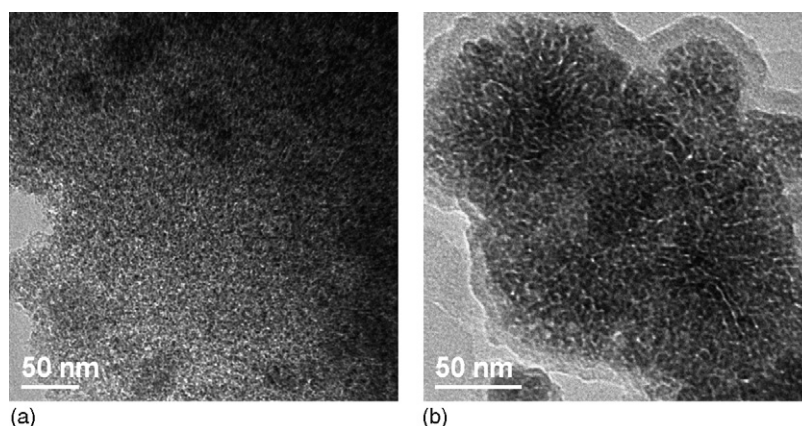

Fig. 3. Typical TEM images of CMM-1/50 (a) and its reversed carbonaceous mesoporous structure (b).
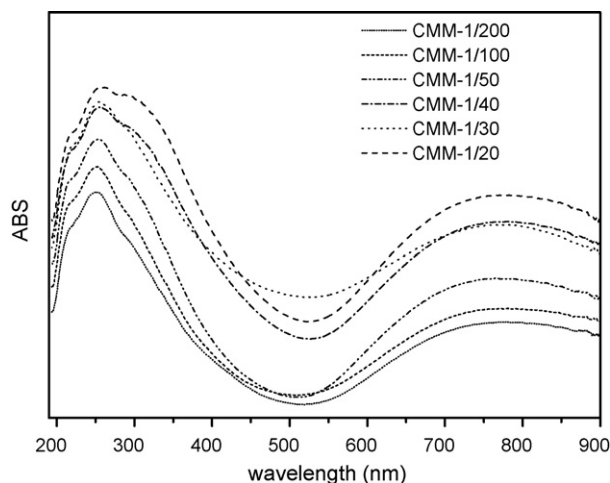
Fig. 4. Diffuse reflectance UV–vis spectra of Cu-incorporated mesoporous materials with different Cu/Si ratios.

activity of CMM-1/50 possibly arises from highly dispersed copper species with relative high content because the activity of the CMMs decreases gradually with increasing amount of crystalline tenorite phase of CuO. Moreover, the molar ratio of hydroquinone/catechol (HQ/CAT) nearly reaches a constant over CMM-1/50 and the distribution of HQ and CAT in the prod-

Table 2
The catalytic activities and selectivity of CMM-*x* and other catalysts in the phenol hydroxylation reaction using H_2O_2 as oxidant[a]

Catalyst	Phenol conversion (%)	H_2O_2 efficiency[b] (%)	Distribution of products[c] (%)		
			HQ	BQ	CAT
CMM-1/20	22.5	67.6	53.9	2.3	43.8
CMM-1/30	23.7	71.2	53.4	1.6	44.9
CMM-1/40	22.0	66.1	53.5	1.5	44.9
CMM-1/50	25.1	75.4	59.5	1.2	39.3
CMM-1/100	20.9	62.8	55.6	1.2	43.2
CMM-1/200	18.4	55.3	54.0	0.6	45.4
TS-1[d]	20.8	62.5	44.4	0.1	55.5
CuO (tenorite)	9.8	29.4	40.9	11.8	47.3

[a] Reaction conditions: 1.0 g phenol, 15 g distilled water as solvent, 50 mg catalyst, 0.36 mL of 30 wt.% H_2O_2 as oxidant, reaction temperature = 343 K, reaction time = 4 h. The molar ratio of phenol:H_2O_2:H_2O is 3:1:239.
[b] H_2O_2 efficiency = 100 (H_2O_2 consumed in the formation of diphenol and benzoquinone, mol)/(total H_2O_2 added, mol).
[c] HQ: hydroquinone; BQ: *para*-benzoquinone; CAT: catechol. The product of tar is not included.
[d] Ti/(Ti + Si) = 0.022.

ucts is contrary to the cases of Cu-SBA-15 and Cu-HMS [16,21]. The dispered copper species within 3D worm-like mesoporous framework may have stronger interaction with CAT, leading to higher selectivity of HQ. To understand the performances of

Table 3
Catalytic activity and selectivity in phenol hydroxylation over CMM-1/50 under different reaction conditions[a]

No.	Conditions		Phenol conversion (%)	Product selectivity (%)		
				HQ	BQ	CAT
1		Water	25.1	59.5	1.2	39.3
2		Acetonitrile	8.3	37.2	29.1	33.7
3	Solvent	Cyclohexane	4.1	53.7	10.8	35.5
4		Ethanol	2.1	78.6	3.4	18.0
5		Acetone	0.6	33.3	45.0	21.7
6		3:40	20.2	58.1	1.5	40.4
7		3:80	21.5	54.6	0.9	44.4
8	Phenol/H_2O[b] (molar ratio)	3:159	21.0	55.2	1.0	43.8
9		3:239	25.1	59.5	1.2	39.3
10		3:318	20.6	53.7	1.0	45.4
11		3:477	20.7	53.6	1.0	45.4
12		293	7.6	40.7	9.4	49.9
13		313	11.2	45.3	7.1	47.6
14	Reaction temperature	323	16.7	51.0	3.4	45.6
15		333	18.4	53.8	1.7	44.5
16		343	25.1	59.5	1.2	39.3
17		1.0	9.9	49.5	3.0	47.5
18		2.5	17.5	51.4	2.3	46.3
19	Catalyst amount (%, w/w phenol)	5.0	25.1	59.5	1.2	39.3
20		7.5	23.7	53.4	1.6	44.9
21		10.0	19.7	51.8	1.5	46.7
22		3:1	25.1 (75.4)[d]	59.5	1.2	39.3
23		2:1	24.9 (49.8)[d]	51.8	1.2	47.0
24	Phenol/H_2O_2[c] (molar ratio)	1:1	28.5 (28.5)[d]	49.5	1.4	49.1
25		1:2	37.7 (18.9)[d]	49.9	0.5	49.6
26		1:3	43.9 (14.6)[d]	48.3	1.1	50.6

[a] Except the tested conditions, the other conditions are the same as those in Table 2.
[b] The molar ratio of phenol/H_2O is changed by varying the amount of water.
[c] The molar ratio of phenol/H_2O_2 is changed by varying the amount of H_2O_2.
[d] The data in the parentheses are the H_2O_2 efficiency.

CMM catalysts, CMM-1/50 was chosen as the catalyst to study the influence of various reaction parameters that affect the catalytic activity and product selectivity.

3.2.2. Influence of solvent

Previous studies showed that solvent had a profound effect on phenol hydroxylation when TS-1 or TS-2 was used as catalyst [32,33]. The solvent influence on phenol hydroxylation over CMM-1/50 is shown in Table 3 (Nos. 1–5). When acetone, ethanol, cyclohexane, or acetonitrile is used as a solvent, phenol conversion of 0.6%, 2.1%, 4.1% or 8.3% is obtained, respectively, although acetone was reported the best solvent for phenol hydroxylation over TS-1 catalyst [32]. When water is employed as a solvent, the phenol conversion over CMM-1/50 increases significantly to 25.1% compared to the organic solvents. The effect of the amount of water on the reaction is also investigated (Table 3, Nos. 6–11). The phenol conversion changes little with the phenol/H_2O ratio and an optimal ratio is ca. 0.0126 (3:239).

3.2.3. Influence of reaction temperature

The phenol conversion and product selectivity in reaction temperature range of 293–343 K are listed in Table 3 (Nos. 12–16). Obviously, both of phenol conversion and selectivity to diphenol increase with increasing temperature. At 293 K, phenol conversion is 4.6% with a diphenol selectivity of 90.6%. At 343 K phenol conversion and diphenol selectivity are 25.1% and 98.8%, respectively. Regarding the product distribution, hydroquinone selectivity increases from 40.7% at 293 K to 59.5% at 343 K. However, the reaction temperature above 343 K was not examined because the higher reaction temperature may result in tar formation due to the side reaction of benzoquinone oxidation [34].

3.2.4. Influence of the amount of catalyst

The activity in phenol hydroxylation using different amount of CMM-1/50 catalyst is listed in Table 3 (Nos. 17–21). The phenol conversions are 9.9% and 25.1% when the amount of CMM-1/50 are 1% and 5% (weight ratio of CMM-1/50 catalyst to phenol), respectively. The addition of catalyst over 5% has a negative effect on the phenol hydroxylation, which is different from that of TS-1. It is believed that larger amount of Cu-containing catalyst promotes the decomposition of H_2O_2 to O_2 [6], leading to the decrease of the efficiency of H_2O_2.

3.2.5. Influence of molar ratio of phenol to H_2O_2

The influence of phenol/H_2O_2 ratio in phenol hydroxylation reaction is listed in Table 3 (Nos. 22–26). A higher molar ratio of phenol/H_2O_2 in the reaction leads to high efficiency of H_2O_2. The H_2O_2 efficiency is 76.1% when the molar ratio of phenol/H_2O_2 is 3/1, whereas the H_2O_2 efficiency decreases to 14.6% when the molar ratio is 1/3. Moreover, the lower phenol/H_2O_2 ratio may result in formation of tar by-product [6].

3.2.6. Influence of the reaction time

The hydroxylation activity and product selectivity of CMM-1/50 catalyst at various reaction times are presented in Table 4.

Table 4
Catalytic activity and selectivity in phenol hydroxylation over CMM-1/50 with various reaction time[a]

Reaction time (min)	Phenol conversion (%)	Product selectivity (%)		
		HQ	BQ	CAT
5	13.5	42.6	11.9	45.5
10	16.0	48.1	11.1	40.8
20	17.0	51.7	7.8	40.5
40	19.1	53.8	5.9	40.3
60	19.7	55.4	4.9	39.6
240	20.4	61.0	0.8	38.1

[a] H_2O_2 is added in once to start the reaction. The other reaction conditions are the same as those in Table 2.

A short reaction time results in incomplete conversion of phenol and low diphenol selectivity, and the conversion increases remarkably in the time range of 0–60 min. When the reaction time is 1 h, phenol conversion is 19.7%. With increasing reaction time to 4 h, phenol conversion increases slightly. Compared with the reaction data at 4 h over CMM-1/50 in Table 2, one finds that the methods of adding H_2O_2 result in different catalytic performance, where dropwise addition of H_2O_2 leads to higher diphenol selectivity and yield.

In the phenol hydroxylation over Cu-containing catalysts with different Cu nature and support, a number of similar mechanisms have been proposed [6,16,21,33]. It is believed that the Cu^{2+} species on CMM may first activate H_2O_2 to form $OH^\bullet$ radicals, and then, the $OH^\bullet$ radicals oxidize phenol to dihydrobenzenes. The proposed reaction pathways over CMMs catalyst similar to those over Cu-HMS and Cu-SBA-15 are shown in Scheme 1 [16,21]. The interaction between Cu catalysts and
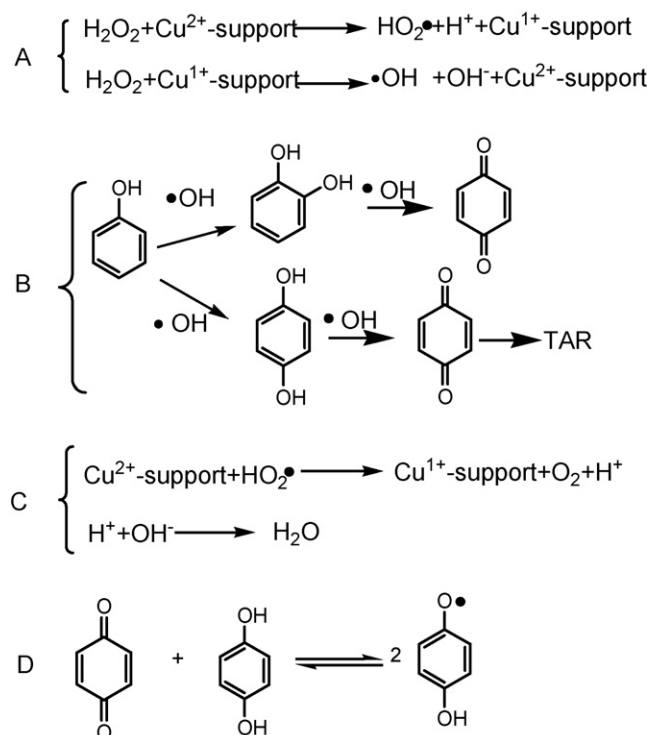
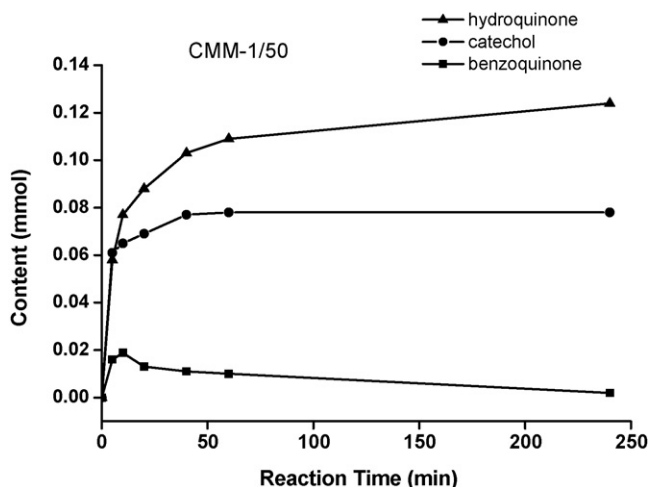Scheme 1. Phenol hydroxylation via a redox mechanism.

Fig. 5. The change of products with reaction time over CMM-1/50.

hydrogen peroxide results in the formation of $HO_2^{\bullet}$ and $^{\bullet}OH$ species, via a redox mechanism (step A). Hydroquinone and catechol are then obtained in parallel processes by the attack of $^{\bullet}OH$ radicals to the aromatic ring and hydroquinone can be oxidized to form benzoquinone and over oxidized product tar (step B). In addition, oxygen and water are formed in side reactions by the decomposition of H_2O_2, resulting in the decrease of H_2O_2 efficiency (step C). By the analysis of the change of products with reaction time over CMM-1/50 in our reaction system, we found that there is a maximum content of benzoquinone at the early reaction stage of ca. 10 min (see Fig. 5 and Table 4). Then, the content of benzoquinone decreases and that of hydroquinone and catechol increase with increasing reaction time, suggesting that there is a balance between the hydroquninone and benzoquinone (step D).

3.2.7. Recycling test of the catalyst

The catalytic results of CMM-1/50 in three runs are listed in Table 5. After second run of phenol hydroxylation, CMM-1/50 catalyst still shows excellent phenol conversion of 24.0%, which is accordance with the low Cu leaching of the catalysts. Phenol hydroxylation activity over catalysts with small surface area, such as $Cu_2(OH)PO_4$ and V–Zr mixed oxide, decreased greatly in their second round catalytic reaction, which is possibly due to the pollution of tar side product on the surface of the catalyst [7]. Cu-SBA-15 with large surface area ($728 \, m^2 \, g^{-1}$) and 1D mesopore structure also showed poor catalytic activity in the

second run of phenol hydroxylation [21]. It can be inferred that the 3D worm-like mesopore structure of Cu-incorporated mesoporous materials is favorable for the mass transferring between catalytic active centers and solution. It also helps to prevent Cu active center from being poisoned by the tar pollutant.

4. Conclusion

A series of novel Cu-incorporated mesoporous materials CMMs were synthesized by a sol–gel method using glutaric acid as template. It was demonstrated that the CMMs had a 3D worm-like mesoporous structure with a large surface area of $600–800 \, m^2 \, g^{-1}$, exhibiting high catalytic activity in the phenol hydroxylation with H_2O_2 comparable to TS-1. Under optimal reaction condition the phenol conversion, the diphenol yield and the efficiency of H_2O_2 reaches 25.1%, 98.8% and 75.4% over CMM-1/50 (reaction time = 4 h), respectively. Moreover, after centrifugation and drying at $40\,^{\circ}C$ for 5 h the recycled catalyst preserves its initial activity.

Table 5
Catalytic activity and selectivity in phenol hydroxylation over CMM-1/50 with various cycles[a]

Reaction cycle[b]	Phenol conversion (%)	Cu leaching after reaction (%)	Product selectivity (%)		
			HQ	BQ	CAT
1	25.1	1.3	59.5	1.2	39.3
2	23.8	2.7	53.0	0.8	46.2
3	24.0	2.9	52.7	1.7	45.6

[a] The other reaction conditions are the same as those in Table 2.
[b] The catalyst was recycled by centrifugation and drying at $40\,^{\circ}C$ for 5 h.

References

[1] J.O. Edwards, R. Curci, in: G. Strukul (Ed.), Catalytic Oxidations with Hydrogen Peroxide As Oxidant, Kluwer Academic Publishers, Dordrecht, 1992, pp. 45–95.
[2] A.L. Eliseev, A.K. Yatsimirskii, React. Kinet. Catal. Lett. 43 (1991) 419.
[3] L.I. Simándi, Dioxygen Activation and Homogeneous Catalytic Oxidation, Elsevier, Amsterdam, 1991.
[4] J.F. Yu, Y. Yang, T.H. Wu, C.C. Sun, Chem. J. Chin. Univ. 17 (1996) 126.
[5] Q.S. Liu, J.F. Yu, Z.L. Wang, P.P. Yang, T.H. Wu, React. Kinet. Catal. Lett. 73 (2001) 179.
[6] F.S. Xiao, J.M. Sun, X.J. Meng, R.B. Yu, H.M. Yuan, J.N. Xu, T.Y. Song, D.Z. Jiang, R.R. Xu, J. Catal. 199 (2001) 273.
[7] R.B. Yu, F.S. Xiao, D. Wang, J.M. Sun, Y. Liu, G.S. Pang, S.H. Feng, S.L. Qiu, R.R. Xu, C.G. Fang, Catal. Today 51 (1997) 39.
[8] K.Z. Zhu, C.B. Liu, X.K. Ye, Y. Wu, Appl. Catal. A: Gen. 168 (1998) 365.
[9] A. Dubey, V. Rives, S. Kannan, J. Mol. Catal. A: Chem. 181 (2002) 151.
[10] V. Ramaswamy, M.S. Krishnan, A.V. Ramaswamy, J. Mol. Catal. A: Chem. 181 (2002) 81.
[11] M. Taramasso, G. Perego, B. Notari, US Patent 4,410,501 (1983).
[12] J.S. Reddy, R. Kumar, P. Ratnasamy, Appl. Catal. 58 (1990) L1.
[13] M.A. Camblor, A. Corma, A. Martinez, J. Perez-Pariente, Chem. Commun. (1992) 589.
[14] J. Wang, J.-N. Park, X.-Y. Wei, C.W. Lee, Chem. Commun. (2003) 628.
[15] W.A. Carvalho, M. Wallau, U. Schuchardt, J. Mol. Catal. A: Chem. 144 (1999) 91.
[16] Z.H. Fu, J.H. Chen, D.L. Yin, D.H. Yin, L.X. Zhang, Y.Y. Zhang, Catal. Lett. 66 (2000) 105.
[17] B.Y. Chou, J.L. Tsai, S.F. Cheng, Micropor. Mesopor. Mater. 48 (2001) 309.
[18] W. Zhao, Y.F. Luo, P. Deng, Q.Z. Li, Catal. Lett. 73 (2001) 199.

[19] C.W. Lee, D.H. Ahn, B. Wang, J.S. Hwang, S.-E. Park, Micropor. Mesopor. Mater. 44 (2001) 587.

[20] Y. Han, X.J. Meng, H.B. Guan, Y. Yu, L. Zhao, X.Z. Xu, X.Y. Yang, S. Wu, N. Li, F.S. Xiao, Micropor. Mesopor. Mater. 57 (2003) 191.

[21] L.P. Wang, A.G. Kong, B. Chen, H.M. Ding, Y.K. Shan, M.Y. He, J. Mol. Catal. A: Chem. 230 (2005) 143.

[22] J.S. Choi, S.S. Yoon, S.H. Jang, W.S. Ahn, Catal. Today 111 (2006) 280.

[23] Y. Ren, L.P. Qian, B. Yue, H.Y. He, Chinese J. Catal. 24 (2003) 947.

[24] N. Ma, Z. Ma, Y.H. Yue, Z. Gao, J. Mol. Catal. A: Chem. 184 (2002) 361.

[25] A.J.H.P. Vanderpol, A.J. Verduyn, J.H.C. Vanhooff, Appl. Catal. A: Gen. 96 (1993) L13.

[26] P.T. Tanev, T.J. Pinnavaia, Science 267 (1995) 865.

[27] K.S.W. Sing, D.H. Everett, R.A.W. Haul, L. Moscou, R.A. Pierotti, J. Rouquérol, T. Siemieniewska, Pure Appl. Chem. 57 (1985) 603.

[28] R. Ryoo, S.H. Joo, S. Jun, J. Phys. Chem. B 103 (1999) 7743.

[29] Z. Shan, E. Gianotti, J.C. Jansen, J.A. Peters, L. Marchese, T. Maschmeyer, Chem. Eur. J. 7 (2001) 1437.

[30] Y. Itho, S. Nishiyama, S. Tsuruya, M. Masai, J. Phys. Chem. 98 (1994) 960.

[31] O.P. Tkachenko, K.V. Klementiev, E. Löffler, I. Ritzkopf, F. Schüth, M. Bandyopadhyay, S. Grabowski, H. Gies, V. Hagen, M. Muhler, L.H. Lu, R.A. Fischer, W. Grünert, Phys. Chem. Chem. Phys. 5 (2003) 4325.

[32] A. Tuel, S. Moussa-Khou Zami, Y. Ben Tarit, C. Naccache, J. Mol. Catal. 68 (1991) 45.

[33] J.S. Reddy, S. Sivasanker, P. Ratnasamy, J. Mol. Catal. 71 (1992) 373.

[34] C.B. Liu, Z. Zhao, X.G. Yang, X.K. Ye, Y. Wu, Chem. Commun. (1996) 1019.